

Energy Efficient Exact and Approximate Systolic Array Architecture for Matrix Multiplication

Pragun Jaswal, L.Hemanth Krishna, Srinivasu Bodapati
Indian Institute of Technology, Mandi,
thepragun@gmail.com, hemanth.krishna412@gmail.com, srinivasu@iitmandi.ac.in

Abstract—Deep Neural Networks (DNNs) require highly efficient matrix multiplication engines for complex computations. This paper presents a systolic array architecture incorporating novel exact and approximate processing elements (PEs), designed using energy-efficient positive partial product and negative partial product cells, termed as PPC and NPPC, respectively. The proposed 8-bit exact and approximate PE designs are employed in a 8x8 systolic array, they achieve energy savings of 22% and 32%, respectively, compared to the existing design. To demonstrate their effectiveness, the proposed PEs are integrated into a systolic array (SA) for Discrete Cosine Transform (DCT) computation, achieving high output quality with a PSNR of 38.21 dB. Furthermore, in an edge detection application using convolution, the approximate PE achieves a PSNR of 30.45 dB. These results highlight the potential of the proposed design to deliver significant energy efficiency while maintaining competitive output quality, making it well-suited for error-resilient image and vision processing applications.

Index Terms—Approximate Computing, Systolic Array, Matrix Multiplication, Processing Element, Low Power Design, DCT, Edge Detection

I. INTRODUCTION

Artificial Intelligence (AI) and Machine Learning (ML) have become integral to a wide range of applications, including computer vision, natural language processing, speech recognition, and autonomous systems [1], [2]. At the core of these workloads are deep neural networks (DNNs), which rely extensively on large-scale matrix multiplications to perform computations across multiple layers of interconnected neurons. Both the training and inference phases of DNNs involve billions of multiply-accumulate (MAC) operations, making matrix multiplication one of the most computationally and energy-intensive kernels in modern AI accelerators [3].

Systolic arrays (SAs) have emerged as an effective hardware architecture for accelerating matrix multiplications [4]. Recent advances in domain-specific hardware, such as Google’s Tensor Processing Unit (TPU), have demonstrated the ability of systolic arrays to deliver high throughput for DNN workloads. However, conventional systolic arrays typically employ exact arithmetic units, which incur significant energy consumption and large silicon area overheads. These limitations hinder their deployment in resource-constrained platforms, such as edge devices and Internet of Things (IoT) systems, where energy efficiency is of paramount importance. To mitigate these challenges, approximate computing has been widely explored as a design paradigm that trades exactness for improvements in energy efficiency and hardware complexity.

In this paper, we propose both exact and approximate processing element that supports both signed and unsigned operations for systolic array-based matrix multiplication. The proposed PE significantly reduces hardware complexity and energy consumption while maintaining acceptable computational accuracy. This makes it well-suited for error-tolerant applications such as image processing and machine learning, where efficiency is prioritized over exact precision. The major contributions of this paper are summarized as follows:

- Proposed an energy-efficient approximate systolic array architecture for matrix multiplication, introducing novel exact and approximate Processing Elements (PEs).
- Proposed approximate Positive Partial Product Cell (PPC)s and Negative Partial Product Cell (NPPC)s, these blocks achieve 46.8% and 38.7% of energy savings respectively as compared to the best existing design [5].
- Proposed exact signed 8-bit PE achieves 20.26% of energy saving over the design [6], while the proposed approximate signed 8-bit PE achieves 13.11% of energy saving over the design [5].
- Validation of the proposed architecture on two applications: DCT for image compression and convolution-based edge detection, results have found to achieve a PSNR of 45 dB for DCT, 30.45 dB for edge detection.

The rest of the paper is organized as follows. Section II explains the matrix multiplication using systolic array architecture. Section III presents the proposed processing elements for the matrix multiplication. Sections IV and V present the results and applications, respectively. The conclusions are presented in Section VI.

II. SYSTOLIC ARRAY BASED MATRIX MULTIPLICATION ARCHITECTURE

Matrix multiplication plays a major role in accelerating the applications such as machine learning, signal processing, and neural networks. Several systolic array architectures for matrix multiplication are found in literature [7]–[9]. Recently, with applications in neural networks with larger data, GEMM-based matrix multiplication using a systolic array is highly appreciated for machine learning applications [10], [8].

The latency of the conventional systolic array architecture, illustrated in Fig. 1, is given by $3N - 2$ clock cycles [11].

In a conventional systolic array as shown in Fig. 1, the processing element (PE) is the basic block for executing multiply-accumulate (MAC) operations [9]. Since a large number of

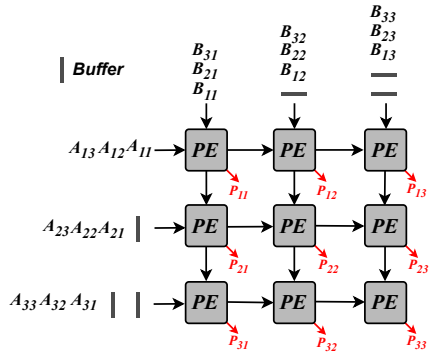


Fig. 1. Architecture of 3×3 Systolic Array for Matrix Multiplication [7].

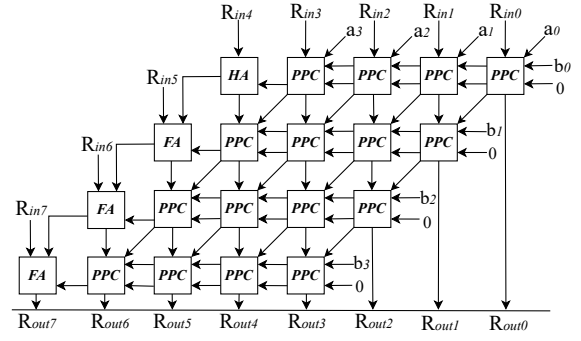


Fig. 4. Proposed Exact 4-Bit Unsigned PE Design

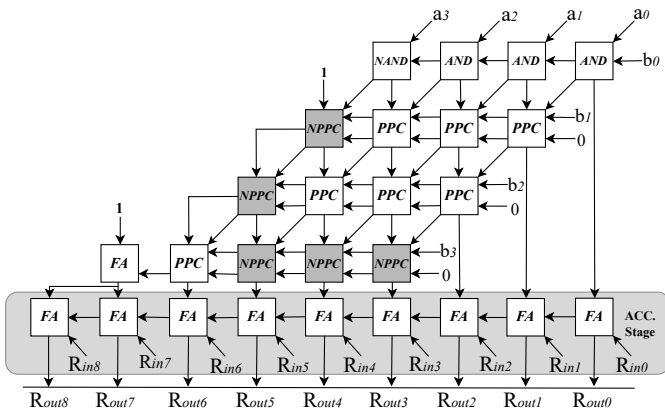


Fig. 2. Existing Design of Exact 4-Bit Signed PE [6]

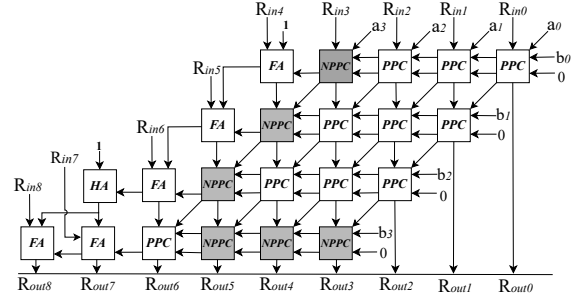


Fig. 5. Proposed Exact 4-Bit Signed PE Design

III. HARDWARE IMPLEMENTATION OF PROPOSED PROCESSING ELEMENT (PE)

First, we present the exact PE architecture using the proposed optimized PPC and NPPC cells.

A. Proposed Exact Processing Element

The proposed PE architecture eliminates the conventional separation between multiplication and accumulation by integrating them in a single processing element to perform $a \times b + c$. This fused approach enables simultaneous reduction of both partial products and the accumulated sum, improving efficiency and reducing delay. Fig. 4 illustrates the exact 4-bit unsigned PE. In this architecture, PPC play a crucial role in performing the MAC operation. The proposed PPC for the PE are shown in Fig. 6 (a).

PEs operate concurrently, it has a critical impact on the overall performance, energy efficiency, and area utilization. In the conventional design, a PE typically consists of a single multiplier followed by an adder to perform the multiply-accumulate (MAC) operation [9]. Alternatively, some studies optimize the PE by employing Positive Partial Product Cells (PPC) and Negative Partial Product Cells (NPPC) [6], to generate positive partial products and negative partial products, respectively, for enabling efficient signed multiplication as presented in Fig. 2. The partial products are then accumulated using full adders (FA) in the accumulation stage. Fig. 3 illustrates the exact PPC and NPPC blocks used to perform the bit-wise MAC operations.

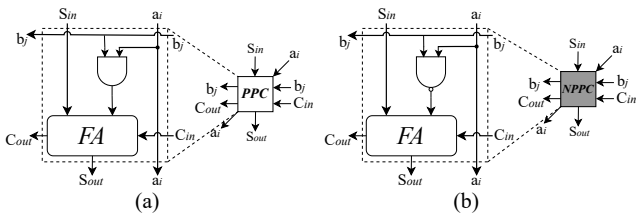


Fig. 3. Conventional approach of Exact (a) PPC and (b) NPPC

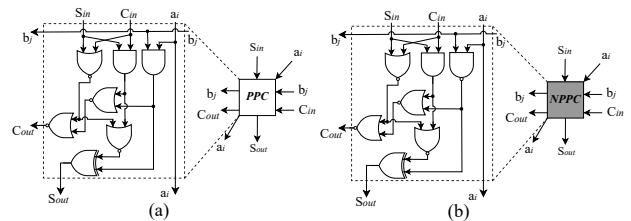


Fig. 6. Proposed exact designs of (a) PPC and (b) NPPC

The next section presents the proposed processing elements for performing the matrix multiplication.

Fig. 5 and 7 illustrates the exact 4 bit and 8-bit signed PE architecture, respectively. The NPPC cells play a crucial role in handling signed operations, and the proposed cell is

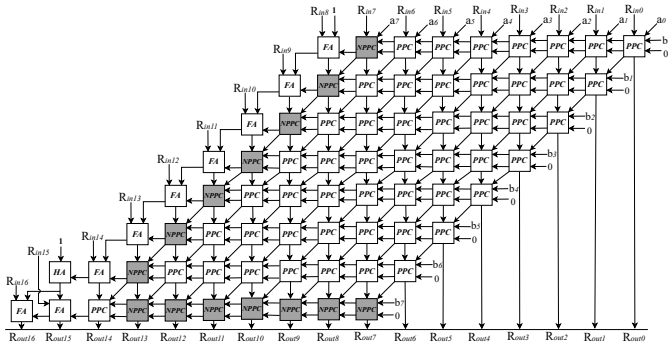


Fig. 7. Proposed exact 8-bit signed PE Design

shown in Fig. 6 (b). For the 8-bit PE, a total of 14 NPPC cells and 50 PPC cells are required, whereas the existing work in [6] requires 15 number of additional full adders as well. In general, for an N -bit PE, the implementation requires $N^2 - 2N - 2$ PPC cells and $2N - 2$ NPPC cells.

B. Proposed Approximate Processing Element

In the proposed design, the PE is constructed using approximate PPC and NPPC blocks. Fig. 8 illustrates the architecture of the proposed approximate 4-bit signed PE, where the dotted blocks represent the approximate PPC and NPPC units. The proposed approximate PPC and NPPC are presented in Fig. 9, and their truth tables are provided in Table I.

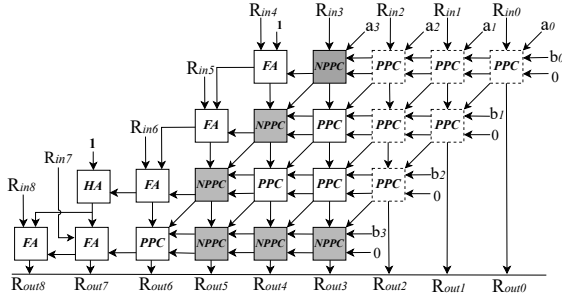


Fig. 8. Proposed Approximate 4-Bit Signed PE Design

The Boolean expression for the *Sum* output of the proposed approximate PPC cell is $S_{out} = (S_{in} + C_{in}) + (a_i \cdot b_i)$, while the corresponding carry output is $C_{out} = a_i \cdot b_i$. For the NPPC block, the *Sum* output is expressed as $S_{out} = (S_{in} + C_{in}) \cdot (a_i \cdot b_i)$, and the carry output is given by $C_{out} = (S_{in} + C_{in}) \cdot (a_i \cdot b_i)$. The proposed approximate PPC introduces five erroneous outputs, out of a total of 16 cases, resulting in an error rate of 5/16. The error occurs for the following combinations of inputs, $(a_i, b_i, S_{in}, C_{in})$ are $(0, 0, 1, 1)$, $(0, 1, 1, 1)$, $(1, 0, 1, 1)$, $(1, 1, 0, 0)$, and $(1, 1, 1, 1)$. The corresponding error probabilities (P_E) for these cases are 9/256, 3/256, 3/256, 9/256, and 1/256, respectively. Therefore, the total error probability of the proposed PPC and NPPC blocks is 25/256.

IV. RESULTS AND DISCUSSION

This section presents hardware evaluation of the proposed and existing designs in terms of area, power, and delay

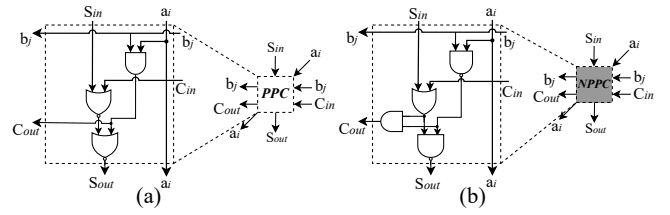


Fig. 9. Proposed Approximate designs of (a) PPC and (b) NPPC

TABLE I
TRUTH TABLE FOR PARTIAL PRODUCT CELL (PPC) AND NEGATIVE PARTIAL PRODUCT CELL (NPPC)

Inputs				PPC: $a \cdot b + C_{in} + S_{in}$			NPPC: $a \cdot b + C_{in} + S_{in}$		
				Exact		Approx	Exact		Approx
a_i	b_i	C_{in}	S_{in}	S	C	S	C	ED	
0	0	0	0	0	0	0	0	0	
0	0	0	1	1	0	1	0	0	
0	0	1	0	1	0	1	0	0	
0	0	1	1	0	1	1	0	-1	
0	1	0	0	0	0	0	1	0	
0	1	0	1	1	0	1	0	0	
0	1	1	0	1	0	1	0	0	
0	1	1	1	0	1	1	0	-1	
1	0	0	0	0	0	0	1	0	
1	0	0	1	1	0	1	0	0	
1	0	1	0	1	0	1	0	0	
1	0	1	1	0	1	1	0	-1	
1	1	0	0	1	0	0	1	0	
1	1	0	1	0	1	0	1	0	
1	1	1	0	0	1	0	1	0	
1	1	1	1	1	1	0	1	-1	

using the Cadence Genus synthesis solution. In addition, error metrics are analyzed through a Python-based simulations.

A. Hardware Evaluation

The existing and proposed designs are designed using Verilog HDL, and then the designs are synthesized using the Cadence Genus Synthesis solution using a 90-nm UMC technology. The synthesized results were then evaluated based on three primary hardware metrics: critical path delay, power consumption, and area, as summarized in Table II for the proposed PPC and NPPC. The analysis shows an energy improvement of 6.4% for the exact design [6], and a significant 46.8% improvement for the proposed approximate PPC design compared to the best existing design [12].

Table III presents the analysis of the proposed and existing PEs for both unsigned and signed designs. The results indicate that the proposed exact PEs achieve superior efficiency compared to existing exact designs, with notable reductions in area, power, and delay, leading to overall improvements of up to 16%. Table III also includes PE designs without PPC and NPPC blocks [13], [14]. A significant improvement in the Power Area Delay Product (PADP) of 65.45% is observed when compared to the design in [13], highlighting that PPC and NPPC based PE designs are highly efficient in terms of hardware metrics. Furthermore, the proposed approximate PE

TABLE II
HARDWARE ANALYSIS OF PROPOSED AND EXISTING PPCS AND NPPCS

Design	PPC				NPPC			
	Area (μm^2)	Power (μW)	Delay (ps)	PDP (aJ)	Area (μm^2)	Power (μW)	Delay (ps)	PDP (aJ)
Exact [6]	25.81	1.03	262	269.86	24.92	0.99	238	235.62
Prop Ext	24.98	0.99	255	252.45	23.47	0.99	216	213.84
Design [6]	13.32	0.64	187	119.04	12.54	0.61	156	95.16
Design [12]	14.13	0.58	157	91.06	13.22	0.60	148	88.80
Prop Apx	10.19	0.44	110	48.4	9.40	0.37	147	54.39

TABLE III
HARDWARE ANALYSIS OF PROPOSED AND EXISTING PROCESSING ELEMENTS

PE Design	Bit Width	Unsigned				Signed			
		Area (μm^2)	Power (μW)	Delay (ns)	PADP ($\times 10^3$)	Area (μm^2)	Power (μW)	Delay (ns)	PADP ($\times 10^3$)
Exact PPCs and NPPCs based Designs									
Design [6]	4	435.9	29.4	1.87	23.96	446.5	29.7	1.65	21.82
	8	1718.5	181.3	3.92	1222.57	1708	183.4	3.71	1162.39
Design [5]	4	432.8	30.4	1.76	23.13	445.3	31.7	1.55	21.88
	8	1730.6	185.3	3.67	1175.71	1716	190.3	3.22	1050.21
Proposed	4	411	26.6	1.73	18.91	419	26.8	1.52	17.06
	8	1659.2	180.7	3.65	1094.33	1620.3	170.6	3.18	879.02
Other Exact Designs									
[13]	8	-	-	-	-	1891	481	2.8	2546.7
[14]	8	-	-	-	-	2366	574	2.5	3395.2
Approximate PPCs and NPPCs based Designs									
Design [6]	4	416.30	24.1	1.56	15.64	435.9	29.6	1.69	21.78
	8	1557.5	172.2	3.55	950.04	1546.3	216.0	3.51	1171.47
Design [12]	4	407.68	25.5	1.43	14.85	427.28	31.7	1.61	21.88
	8	1476.2	164.1	3.21	777.51	1465.2	207.9	3.18	966.75
Design [5]	4	412.2	25.8	1.40	14.90	420.1	28.3	1.40	16.64
	8	1012.1	145.5	3.01	442.91	975.5	177.2	2.50	431.93
Proposed	4	375.6	17.1	1.37	8.79	399.3	25.6	1.35	13.79
	8	985.2	125.3	2.71	334.53	869.5	155.2	2.48	334.66

achieve up to 23% improvement in the PADP compared to the best existing approximate design [5].

Table IV summarizes the results for various systolic array (SA) sizes at 250 MHz. Fig. 10 shows up to 5.9% area savings and 12.8% energy savings of the proposed exact design over [6] across various sizes of systolic array. For the 8-bit configuration with a 16×16 SA, the proposed approximate design achieves a 55.9% reduction in PDP compared to the exact design [6] and a 10.5% improvement compared to the best existing approximate design [5]. These results indicate that the proposed approximate designs achieve substantial gains in hardware efficiency, particularly for large systolic arrays, while maintaining competitive accuracy-performance tradeoffs. Fig. 11 compares the PADP across different systolic array sizes, where the proposed approximate design consistently outperforms existing designs [6], [5].

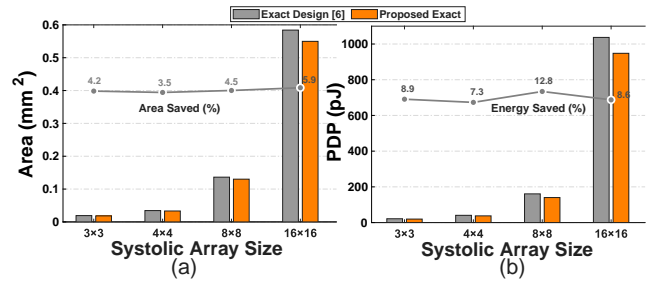


Fig. 10. Area and PDP comparison of the exact design [6] and the proposed design across systolic array sizes.

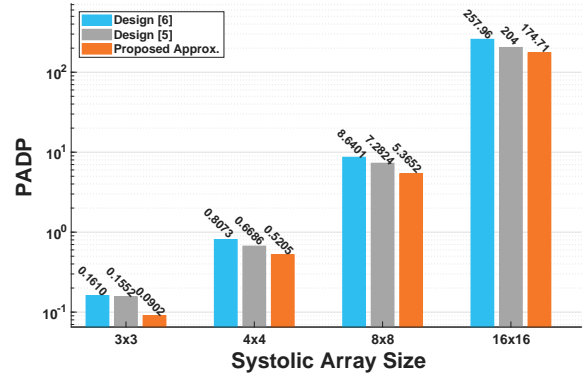


Fig. 11. PADP comparison of existing designs [5], [6] and the proposed approximate design for different systolic array sizes

B. Error Analysis

Accuracy of the proposed approximate MAC design is evaluated using well-known error metrics [15] such as Error Distance (ED), Error Rate (ER), Relative Error Distance (RED), Mean Error Distance (MED), and Mean Relative Error Distance (MRED). These metrics measure the deviation of the approximate outputs from the exact. These metrics are estimated using uniformly distributed input combinations using Python simulations. Table V summarizes the error metrics of 4-bit and 8-bit PE designs. The results indicate that the accuracy of the designs gradually decreases with increasing approximation factor of k , although approximations up to $k = N$ bits still produce acceptable results as discussed in the next section.

As shown in Fig. 12, the proposed approximate design achieves a significant reduction in PDP while maintaining a lower MED compared to existing approximate designs. Although the design in [5] attains a slightly lower MED, the proposed design offers superior area, power, and delay metrics. Furthermore, the proposed exact design demonstrates improved efficiency up to 10% over the exact design [6].

V. APPLICATIONS

In this section, we evaluate the effectiveness of the proposed approximate processing elements (PEs) through three representative applications. The image quality is estimated using metrics such as peak signal to noise ratio (PSNR) and structural similarity index measure (SSIM).

TABLE IV
HARDWARE ANALYSIS OF DIFFERENT DESIGNS FOR VARIOUS SYSTOLIC ARRAY SIZES AT 250 MHZ

Bit Width	Design	3x3				4x4				8x8				16x16			
		Area (mm ²)	Power (mW)	Delay (ns)	PDP (pJ)	Area (mm ²)	Power (mW)	Delay (ns)	PDP (pJ)	Area (mm ²)	Power (mW)	Delay (ns)	PDP (pJ)	Area (mm ²)	Power (mW)	Delay (ns)	PDP (pJ)
4	Exact [6]	0.0062	3.98	1.65	6.57	0.0112	3.98	1.67	6.65	0.0465	17.2	1.88	32.34	0.1901	74.4	2.41	179.30
	Proposed Exact	0.0060	3.90	1.63	6.35	0.0110	3.95	1.64	5.98	0.0459	16.9	1.88	31.77	0.1885	70.7	2.38	168.26
	Approx. [12]	0.0058	3.89	1.62	6.30	0.0105	3.93	1.63	6.40	0.0445	16.8	1.87	31.42	0.1754	65.3	2.38	155.41
	Approx. [6]	0.0056	3.60	1.54	5.54	0.0101	3.90	1.50	5.85	0.0432	15.8	1.86	29.39	0.1600	62.80	2.35	147.58
	Approx. [5]	0.0057	3.80	1.44	5.47	0.0103	3.91	1.30	5.08	0.0440	16.2	1.80	29.16	0.1500	63.00	2.30	144.90
	Proposed Approx.	0.0050	3.31	1.40	4.64	0.0090	3.79	1.27	4.82	0.0407	14.3	1.75	25.19	0.1312	53.92	2.23	120.26
8	Exact [6]	0.0191	6.38	3.36	21.44	0.0345	11.4	3.56	40.58	0.1363	49.8	3.61	179.78	0.5541	265.4	3.91	1037.71
	Proposed Exact	0.0184	6.01	3.25	19.53	0.0333	11.0	3.42	37.62	0.1302	41.1	3.41	140.15	0.5498	242.6	3.91	948.56
	Approx. [12]	0.0155	5.45	2.97	16.19	0.0301	10.4	3.31	34.42	0.1151	35.1	3.02	106.00	0.4424	193.7	3.88	751.556
	Approx. [6]	0.0142	4.20	2.70	11.34	0.0290	9.60	2.90	27.84	0.1050	27.8	2.96	82.29	0.4200	166.0	3.70	614.20
	Approx. [5]	0.0135	4.60	2.50	11.50	0.0285	9.20	2.55	23.46	0.1020	25.5	2.80	71.40	0.4000	150.0	3.40	510.00
	Proposed Approx.	0.0108	3.45	2.42	8.36	0.0269	8.06	2.40	19.35	0.0955	20.5	2.74	56.18	0.3823	139.3	3.28	456.99

TABLE V
ERROR METRICS FOR PROPOSED AND EXISTING PE DESIGNS

Column Wise Approx	Unsigned		Signed	
	NMED	MRED	NMED	MRED
4 bit design				
Prop Apx k=2	0.007	0.091	0.007	0.271
Prop Apx k=3	0.015	0.141	0.015	0.466
Prop Apx k=4	0.030	0.223	0.023	0.642
8 bit design				
Prop Apx k=2	0.0001	0.0011	0.0001	0.0037
Prop Apx k=4	0.0004	0.0033	0.0004	0.0130
Prop Apx k=5	0.0006	0.0075	0.0006	0.0286
Prop Apx k=6	0.0018	0.0108	0.0018	0.0481
Prop Apx k=8	0.0077	0.0328	0.0073	0.2418
Design [6]*	0.00075	0.0082	0.00079	0.0364
Design [12]*	0.00072	0.0075	0.00086	0.0328
Design [5]*	0.00068	0.0068	0.00072	0.0292

*Five columns (k=5) are approximated.

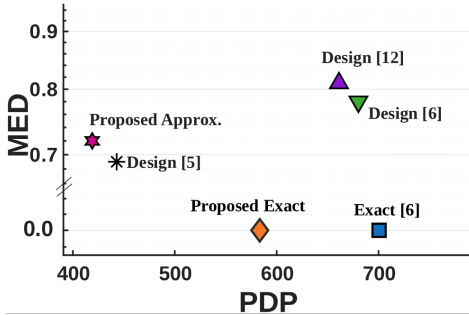


Fig. 12. Comparison of PDP and MED for Signed 8-bit PE.

A. Discrete Cosine Transform (DCT)

It is a widely used mathematical tool in image and video compression standards such as JPEG, and MPEG. In this paper, the proposed processing element (PE) of the systolic array is applied to perform matrix multiplication for an 8×8 two-dimensional integer-scaled DCT. Instead of using floating-point operations, the DCT coefficient matrix is scaled to inte-

ger values [16], making it suitable for hardware architectures that operate on fixed-point or integer arithmetic. This approach reduces hardware complexity, power consumption, and area, while maintaining acceptable image reconstruction quality.

The input image, DCT coefficients, and reconstructed image are shown in Fig. 13. The Peak Signal-to-Noise Ratio (PSNR) and Structural Similarity Index Measure (SSIM) are calculated between the original and reconstructed images. This simulation is implemented in a Python environment and employs an 8×8 systolic array. The output images depicted in Fig. 13 (c) represents the $(N/2 - 2)$ column approximation. As the column-wise approximation parameter k increases, the quality of the output images degrades in terms of PSNR and SSIM as shown in Table VI.

TABLE VI
QUALITY METRICS OF DCT FOR N=8 PROCESSING ELEMENT

k	Column Approx.	PSNR (dB)	SSIM
3	$(N/2 - 1)$	38.21	0.955
4	$(N/2)$	35.67	0.923
7	$(N - 1)$	28.43	0.872

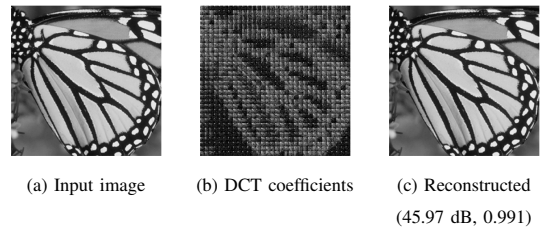


Fig. 13. Resultant images of DCT along with (PSNR and SSIM) values.

B. Edge Detection

Edge detection is a fundamental step in image processing, widely used to extract object boundaries and structural information. Convolution-based operators, such as the Laplacian filter, are commonly employed for this task by emphasizing regions with high spatial intensity variation. In this work, we adopt the 3×3 Laplacian kernel which is particularly effective

for highlighting edges. However, the convolution operation requires multiple signed multiplications between pixel values and filter coefficients, making it computationally intensive.

To address this, the proposed approximate PE is integrated into the convolution process. The design supports different approximation column levels ($k = 3, 4, 5, 6$), where higher values of k correspond to more aggressive approximations. As shown in Table VII, approximation levels of $k = 3$ and $k = 4$ achieve high PSNR values, indicating good image quality. Increasing the approximation level to $k = 5$ and $k = 6$ results in a slight degradation in image quality, but the edge structures remain well preserved while delivering greater hardware efficiency.

TABLE VII
PERFORMANCE OF EDGE DETECTION USING APPROXIMATE SIGNED PROCESSING ELEMENT

Design	Level of Approximation (k)	PSNR (dB)
Proposed	$k = 2$	35.45
	$k = 3$	31.99
	$k = 4$	30.12
	$k = 5$	29.03
Design [17]	$k = 6$	28.41
	$k = 3$	31.78

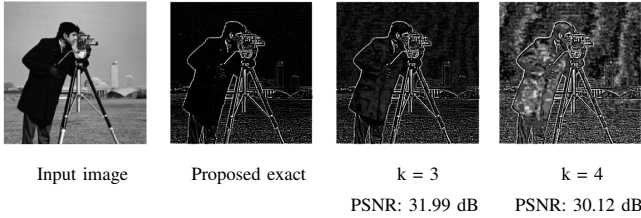


Fig. 14. Edge detection results using the Laplacian filter with the proposed approximate signed PE at different approximation levels.

C. Image Sharpening

Image sharpening enhances edges and fine details by applying convolution with a sharpening kernel. In this work, the proposed approximate PE is integrated to perform the convolution operation, enabling efficient sharpening while reducing computational cost compared to exact designs. Fig. 15 shows the output images obtained from the sharpening operation using the proposed approximate PE. The existing design reported in [17] achieves a PSNR of 27.12 dB.

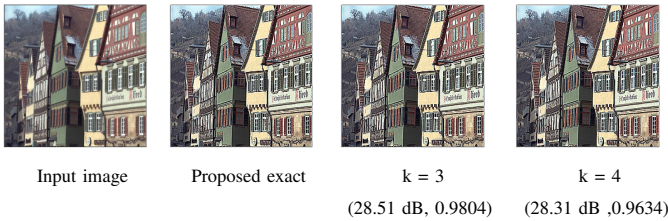


Fig. 15. Image sharpening results using the sharpening filter with the proposed approximate signed PE at different approximation levels, along with (PSNR, SSIM).

VI. CONCLUSION

This work presents an energy efficient systolic array architecture leveraging proposed exact and approximate PE with optimized PPC and NPPC blocks. The proposed designs demonstrate substantial energy savings of up to 32% while maintaining high output quality, validated through applications such as, DCT based image compression, convolution based edge detection and image sharpening. These results highlight the suitability of the architecture for error-resilient image and vision processing tasks, offering a promising balance between performance, energy efficiency, and computational accuracy.

REFERENCES

- [1] Y. LeCun, Y. Bengio, and G. Hinton, "Deep learning," *Nature*, vol. 521, no. 7553, pp. 436–444, 2015.
- [2] I. Goodfellow, Y. Bengio, and A. Courville, *Deep Learning*. Cambridge, MA: MIT Press, 2016.
- [3] S. Mittal, P. Rajput, and S. Subramoney, "A survey of deep learning on cpus: Opportunities and co-optimizations," *IEEE Transactions on Neural Networks and Learning Systems*, vol. 33, no. 10, pp. 5095–5115, 2022.
- [4] A. J. Abdelmaksoud, S. Agwa, and T. Prodromakis, "Dip: A scalable, energy-efficient systolic array for matrix multiplication acceleration," *IEEE Transactions on Circuits and Systems I: Regular Papers*, pp. 1–11, 2025.
- [5] H. Waris, C. Wang, and F. Liu, W. Lombardi, "Axsas: On the design of high-performance and power-efficient approximate systolic arrays for matrix multiplication," vol. 93, no. 6, 2021.
- [6] K. Chen, F. Lombardi, and J. Han, "Matrix multiplication by an inexact systolic array," in *Proceedings of the 2015 IEEE/ACM International Symposium on Nanoscale Architectures (NANOARCH '15)*, 2015, pp. 151–156.
- [7] H. T. Kung, "Why systolic architectures?" *Computer*, vol. 15, pp. 37–46, 1982.
- [8] S. Ortega-Cisneros, "Design and implementation of an noc-based convolution architecture with gemm and systolic arrays," *IEEE Embedded Systems Letters*, vol. 16, no. 1, pp. 49–52, 2024.
- [9] P. J. Varman and I. Ramakrishnan, "Synthesis of an optimal family of matrix multiplication algorithms on linear arrays," *IEEE transactions on Computers*, vol. 35, no. 11, pp. 989–996, 1986.
- [10] K. Inayat and J. Chung, "Hybrid accumulator factored systolic array for machine learning acceleration," *IEEE Transactions on Very Large Scale Integration (VLSI) Systems*, vol. 30, no. 7, pp. 881–892, 2022.
- [11] S. K. Nandigama, H. C. Prashanth, and M. Rao, "Design and evaluation of inexact computation based systolic array for convolution," in *2023 IEEE 14th Latin America Symposium on Circuits and Systems (LASCAS)*, 2023, pp. 1–4.
- [12] H. Waris, C. Wang, W. Liu, and F. Lombardi, "Design and evaluation of a power-efficient approximate systolic array architecture for matrix multiplication," *2019 IEEE International Workshop on Signal Processing Systems (SiPS)*, pp. 13–18, 2019.
- [13] H. Genc, S. Kim, A. Amid, A. Haj-Ali, V. Iyer, P. Prakash, J. Zhao, D. Grubb, H. Liew, H. Mao, A. Ou, C. Schmidt, S. Steffl, J. Wright, I. Stoica, J. Ragan-Kelley, K. Asanovic, B. Nikolic, and Y. S. Shao, "Gemmini: Enabling systematic deep-learning architecture evaluation via full-stack integration," pp. 769–774, 2021.
- [14] M. A. Shafique, K. Inayat, and J. A. Lee, "Csa based radix-4 gemmini systolic array for machine learning applications," 2023.
- [15] J. Liang, J. Han, and F. Lombardi, "New metrics for the reliability of approximate and probabilistic adders," *IEEE Transactions on Computers*, vol. 62, no. 9, pp. 1760–1771, 2013.
- [16] P. K. Meher, S. Y. Park, B. K. Mohanty, K. S. Lim, and C. Yeo, "Efficient integer dct architectures for hevc," *IEEE Transactions on Circuits and Systems for Video Technology*, vol. 24, no. 1, pp. 168–178, 2014.
- [17] A. Kumari and R. P. Palathinkal, "Design and analysis of energy efficient approximate multipliers for image processing and deep neural network," *IEEE Transactions on Circuits and Systems I: Regular Papers*, vol. 72, no. 2, pp. 854–867, 2025.